ALIGNMENT OF OPTIC NERVE HEAD OPTICAL COHERENCE TOMOGRAPHY B-SCANS IN RIGHT AND LEFT EYES

Marzieh Mokhtari[1], Hossein Rabbani[1, 2], Alireza Mehri-Dehnavi[1, 2]
[1]Biomedical Engineering Dept., Faculty of Advanced Medical Technology, Isfahan University of Medical Sciences, Isfahan, Iran
[2]Medical Image & Signal Processing Research Center, Isfahan Univ. of Medical Sciences, Isfahan, Iran

ABSTRACT

Symmetry analysis of right and left eyes can be a useful tool for early detection of eye diseases. In this study, we want to compare the Optical Coherent Tomography (OCT) images captured from optic nerve head (ONH) of right and left eyes. To do this, it is necessary to align the OCT data and compare equivalent B-scans in right and left eyes. For this reason, since the fovea-ONH axes in OCT data are not available due to small field of view in OCT, at first the projection of OCT data of each eye is registered to its corresponding fundus image using extracted vessels by Hessian analysis of directional curvelet subbands. Then, by alignment of fundus images of right and left eyes according to their automatically detected fovea-ONH axes, OCT projections are also aligned. After alignment of OCT projections, aligned B-scans are estimated and used for comparing different parameters such as cup-to-disk ratio (CDR). Using aligned B-scans, two signals of CDRs are obtained from two eyes which each point in these signals corresponds to CDR in a specific part of ONH, i.e., a point-to-point comparison between CDRs of right and left eyes is provided which has potential to lead to a new imaging biomarker for eye disease detection.

Keywords— Symmetry analysis, Cup to Disk Ratio, Registration, Optical coherence tomography, Fundus image, alignment

1. INTRODUCTION

Asymmetry analysis is an appropriate tool for early diagnoses of eye diseases like glaucoma [1-3]. In [3] the authors suggest that we have similar sized optic disk (OD) cups in healthy population and therefore cup-to-disk ratios (CDRs) would be similar in both eyes. However, the presence of an asymmetry in the optic cup size in discs of similar size may be a sign of glaucomatous. Asymmetry analysis on OD parameters such as vertical optic disc diameter and vertical optic CDR was investigated in [1] and three groups of normal population, people having ocular hypertension (OH), and people having open-angle glaucoma (OAG) were compared. These works are based on comparing retinal color fundus images while more detailed information can be obtained by comparing captured images from eyes using other modalities such as Optical Coherent Tomography (OCT). OCT is a non-invasive imaging modality developed for many clinical applications such as diagnosis of ocular diseases [4, 5]. The cross-sectional images of the retina obtained from OCT systems, namely B-scans, is a useful tool for analysis of intra-retinal layers and retinal morphology [6]. Although these B-scans produce a three-dimensional retinal image which provide invaluable information for physicians in diagnosis and monitoring of ocular diseases, analyze these data is a subjective process which cannot be performed quickly and accurately by clinicians. Therefore automatic OCT image analysis has been of a great interest during current years [7-9].

Till now only a few studies for symmetricity analysis in OCT images of right and left eyes have been reported [10-25] . For example in [11] the symmetricity of the retinal nerve fiber layer thickness (RNFLT) between the right and left eye in normal subjects was performed and the most important discrepancy area in RNFL was obtained [11]. In [10], the symmetricity of macular nerve fiber layer (NFL), and optic disk measurements in healthy children was investigated. Most of these works perform their comparison between OCTs without using any automatic alignments between OCTs[12] ,in addition their analysis is limited mostly around macula. In this work we want to automatically align optic nerve head (ONH) OCTs of right and left eyes and estimate the equivalent B-scans of OCT data in center of ONH in individual eyes. This work is useful for comparing CDRs as an important descriptor to investigate the symmetry in two eyes. Using aligned B-scans, two signals of CDRs are obtained which each point in these signals corresponds to CDR in a specific part of ONH in aligned eyes. So, a point-to-point comparison between CDRs of right and left eyes is provided.

Since the fovea-ONH axes in ONH OCT are not available (macula is not detectable in ONH OCT), we need to expand the field of view and use fovea-ONH axes for OCT alignment. For this purpose, it is necessary to register OCT data to fundus image and align the left and right fundus images according to position of macula center and optic disk center. This step is performed by registration of extracted vessels from OCT projection and corresponding fundus image in each eye.

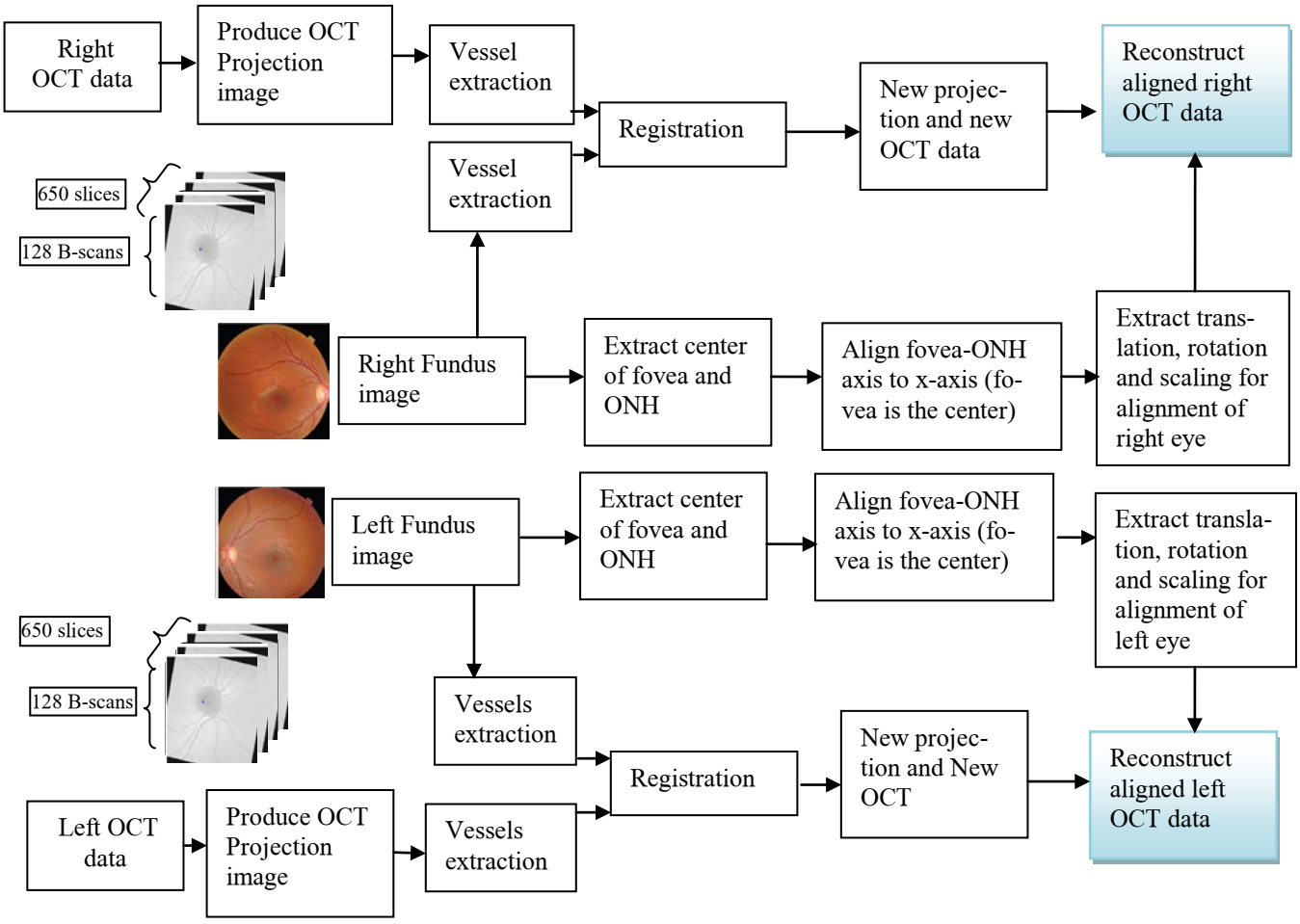

Figure 1: The proposed algorithm for alignment of OCTs in right and left eyes

The paper is organized as follows. Section 2 describes our method. In Section 3 the results are presented and finally this paper is concluded in Section 4.

2. METHOD AND MATERIAL

2.1 MATERIALS

In this paper the OCT data from ONH were collected by a Topcon model of 3D-1000 unit of Feyz Eye Hospital, Isfahan. Their dimensions are 650×512×128 and their resolutions are 125µm×3.25µm×7µm. Then the .FDS files are converted to .MAT file using OCT-EXPLORER software. Fundus images are two-dimensional and their sizes are 1536×1612. These data are from normal subjects that they must have the specifics characteristics. Its specs are:

1- Visual acuity is over 0.6.
2- Power spherical is less than 0.3 diopter.
3- Intraocular pressure (IOP) is less than 21 mm Hg.
4- The subjects don't have Family history of glaucoma and ocular injuries.
5- The CDR is less than 0.6.
6- Free of ocular and systemic disease that can affect the retinal layers for example diabetes mellitus, high blood pressure, etc.

2.2 Proposed Method

The purpose of this paper is estimating the equivalent B-scans in two eyes. The flowchart of our algorithm is shown in Figure 1. The aligned OCTs can be used for calculating and comparing the clinical features such as CDRs in B-scans of two eyes.

In this section, the steps used for estimating the equivalent B-scans is explained. To estimate aligned B-scans, it is necessary to align the OCT data of left and right eyes. OCT data is aligned by aligning fovea-ONH axes. Since the field of view in OCT data doesn't cover both fovea and ONH, we align OCT data by the help of fundus image. For this reason, we focus on two parallel processes, first, alignment of fundus images of eyes, then registration of fundus image with its corresponding OCT projection.

2.2.1 Registering fundus image with projection of OCT

The first step is linking OCT data to fundus image. To do this, it is necessary to connect multimodality data. So, in the first step, the enface presentation of OCT (projection of OCT) is registered to fundus image. Then, all 2D slices in 3D OCT which are parallel to this projection would be changed using the obtained registration parameters for projection image.

Registering the OCT data with fundus image removes moving artifacts in one eye and represents the true position of B-scans in fundus image. So, improvement of blood vessel position can be seen in the fundus image by registering enface representation of B-scans [26]. Object-based features (such as line intersections, edges, contours) are used for multimodality image registration. Blood vessels can be used to extract stable and common features from fundus and OCT images. Similarity functions such as correlation function, Fourier transformation and mutual information are used to match extracted features in both modalities [27]. In this paper we use the multi-step correlation function to register blood vessels of fundus image and projection of OCT data. This similarity function just uses the pattern of blood vessels, so, the processing is fast and accurate, i.e. different kinds of noise do not disturb our registration.

For vessel extraction, Hessian analysis of directional curvelet sub-bands is performed [28]. In this method, curvelet sub-bands are extracted, and then vessel centerlines in each sub-band are segmented by using intensity feature and analyzing eigenvalues. After that, the vessel of selected sub-bands are combined together and false detected vessels are removed [28]. The curvelet transform decomposes the input image to multi-directional outputs, so, it can extract the thin and low contrast vessels in each direction [29]. Now the extracted vessels are fed to similarity function to show the best shift, rotation and scaling as follows:

a. The OCT projection image is scaled around a proximate amount (that is 256×256 for our data-set) and for each size the correlation image is obtained. The maximum pixel of each correlation image shows the best position of OCT projection for that scale, and the maximum of maximum pixels (for all scales) represents the best scaling for registration.

b. After finding the best scale for OCT projection image, the obtained image is rotated from -15 to 15 degree and for each degree the correlation image is calculated. The maximum pixel of each correlation image shows the best position of OCT projection for that degree, and the maximum of maximum pixels (for all degrees) represents the best rotation for registration.

The result of mentioned registration process is shown in Figure 2 for a sample data. In this figure the fundus images and OCT data are registered with extracting vessels of them. The white vessels show matching points. In the overlap region in two images the vessels are registered together well.

2.2.2 Alignment of fundus images of left and right eyes

2.2.2.1 Finding the center of macula and ONH

The first step for aligning two fundus images is, selecting the base points for alignment. For this purpose, the center of macula and ONH are chosen. These points are selected using the intensity features , i.e., the macula center is found by searching darkest pixel in center of image and the initial estimate of center of ONH is obtained by searching the brightest pixel in fundus image. The estimated center of ONH can be improved using active contour [30]. We can detect disk edge with level set method and find the center of disk contour. For this algorithm we select the window around brightest pixels as initial contour.

2.2.2.2 Aligning Fovea-ONH axes with horizontal line

After finding the center of fovea and ONH, the fovea-ONH axes of both images are aligned to horizontal line. Then, the fundus image and accordingly registered OCT projection to fundus image, are rotated around the center of macula. So, the left and right OCT projection images, which are registered to fundus images, would be aligned.

2.2.3 Alignment of right and left B-scan OCT data.

For aligning B-scan OCT data of right and left eyes, the parallel slices to OCT projection image of each eye are aligned by using the same parameters obtained for OCT projection image. Therefore all 650 B-scans with dimension of 512×128 would be changed so that the new B-scan OCTs will be registered with aligned fundus images. After aligning we can present the equivalent B-scan that are parallel with fovea-ONH axis. Figure 3 shows the corresponding B-scans in left and right eyes before, and after alignment for a sample data.

3. RESULTS

The OCT data from ONH of right and left eyes collected by a Topcon model of 3D-1000 unit were aligned according to proposed method in Figure 1. Using this algorithm we can compare the corresponding B-scans before and after alignment visually. Figure 3 shows that 2 corresponding B-scans before and after alignment. After alignment we can compare clinical features extracted from corresponding aligned B-scans in both eyes. For example, by each B-scan we can estimate CDR in a specific region (such as orange and blue area in ONH in Figure 3.a and 3.b) and compare the CDRs in two eyes in this specific area (Figure 4). There are different CDR definitions. In this paper, we use the cup and disk boundary that is presented by Yu-ping Wang, et. al [31]. Using this definition for aligned B-scans, two signals of CDRs are obtained from two eyes which each point in these signals corresponds to CDR in a specific part of ONH, i.e., a point-to-point comparison between CDRs of right and left eyes is provided which has potential to lead to a new imaging biomarker for eye disease detection.

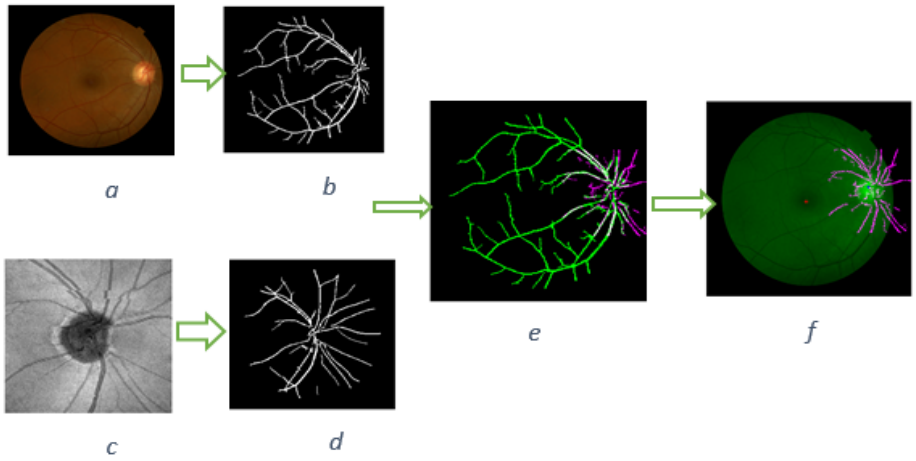

Figure 2: Registration of projection of OCT data with fundus image. b and d are extracted vessels from fundus and OCT projection images a and c. e and f are the results of registration.

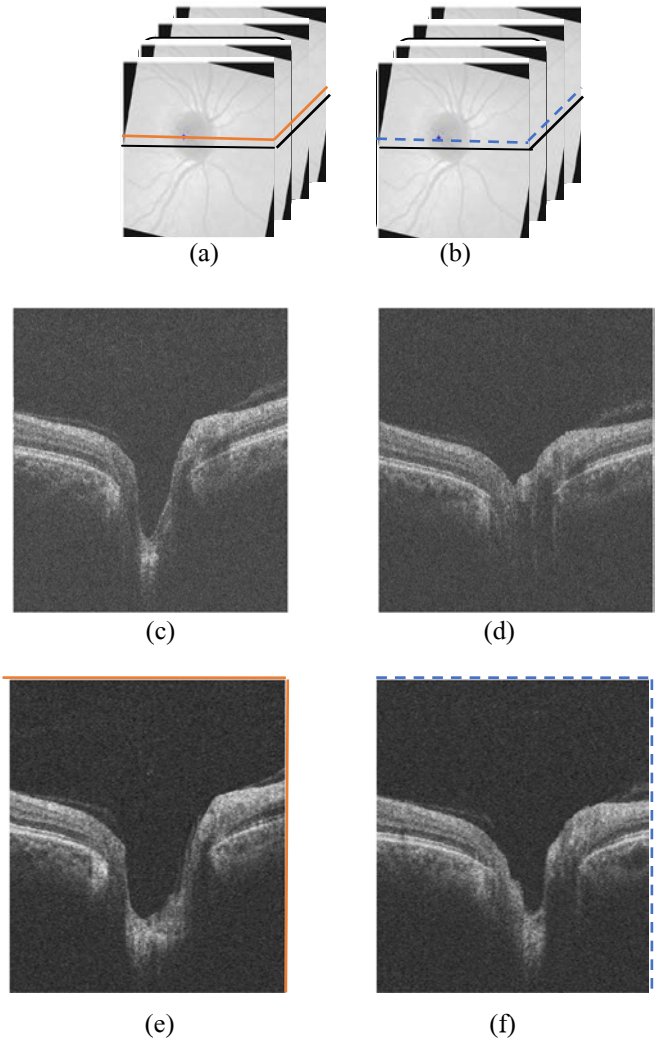

Figure 3: a and b show right and left aligned OCT data, c and d show corresponding B-scans in left and right eyes before alignment, e and f show corresponding B-scans in left and right eyes after alignment.

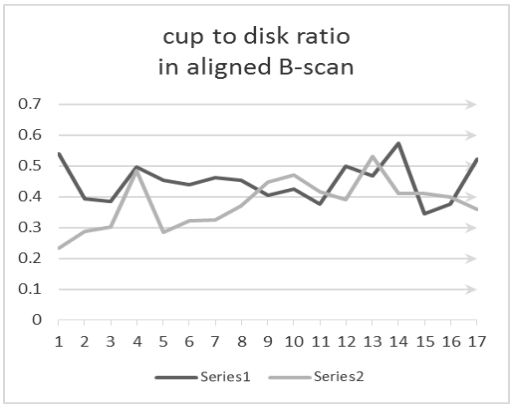

Figure 4: The local cup to disk ratio in left and right eyes of a sample data (for 17 aligned B-scan)

4. Conclusion

In this paper, a fast algorithm for estimating aligned B-scans in right and left eyes was proposed. For this reason, at first projection of OCT data and fundus images are registered. Then the left and right fundus images are aligned based on fovea-ONH axes. Finally, the corresponding B-scans in left and right eyes are aligned using aligned fundus images and registered OCT projection images with their corresponding fundus images. We used this approach to compare the clinical features in both eyes such as local cup-to-disc ratio which can be used to extract similarity indexes between right and left eyes (for comparing normal and abnormal subjects). We can use active contour [30] to segment ONH and calculate the center of ONH, also extract the foveal avascular zone (FAZ) [32] and obtain the macula. Using these methods for finding macula and center of ONH we anticipate to have improved results for alignment of B-scans in right and left eyes. The proposed method for calculating cup-to-disc ratio from each B-scan can be improved by using least-square and sparse signal restoration methods such as split augmented Lagrangian shrinkage algorithm (SALSA) [33].

5. REFERENCES

[1] L. S. Ong, P. Mitchell, P. R. Healey, and R. G. Cumming, "Asymmetry in optic disc parameters: the Blue Mountains Eye Study," *Investigative ophthalmology & visual science,* vol. 40, pp. 849-857, 1999.

[2] J. Jonas, R. Thomas, R. George, E. Berenshtein, and J. Muliyil, "Optic disc morphology in south India: the Vellore Eye Study," *British journal of ophthalmology,* vol. 87, pp. 189-196, 2003.

[3] R. Ramakrishan, R. Krishnadas, A. L. Robin, and M. Khurana, *Diagnosis and Management of Glaucoma*: JP Medical Ltd, 2013.

[4] I. Ghorbel, F. Rossant, I. Bloch, S. Tick, and M. Paques, "Automated segmentation of macular layers in OCT images and quantitative evaluation of performances," *Pattern Recognition,* vol. 44, pp. 1590-1603, 2011.

[5] M. K. Garvin, M. D. Abràmoff, R. Kardon, S. R. Russell, X. Wu, and M. Sonka, "Intraretinal layer segmentation of macular optical coherence tomography images using optimal 3-D graph search," *IEEE Transactions on Medical Imaging,* vol. 27, pp. 1495-1505, 2008.

[6] G. Quellec, K. Lee, M. Dolejsi, M. K. Garvin, M. D. Abràmoff, and M. Sonka, "Three-dimensional analysis of retinal layer texture: identification of fluid-filled regions in SD-OCT of the macula,"*IEEE Transactions on Medical Imaging,* vol. 29, pp. 1321-1330, 2010.

[7] R. Kafieh, H. Rabbani, M. D. Abramoff, and M. Sonka, "Intra-retinal layer segmentation of 3D optical coherence tomography using coarse grained diffusion map," *Medical image analysis,* vol. 17, pp. 907-928, 2013.

[8] R. Kafieh, H. Rabbani, and I. Selesnick, "Three Dimensional Data-Driven Multi Scale Atomic Representation of Optical Coherence Tomography," *IEEE Transcations on Medical Imaging*, 2014. doi: 10.1109/TMI.2014.2374354

[9] R. Kafieh, H. Rabbani, and S. Kermani, "A review of algorithms for segmentation of optical coherence tomography from retina," *Journal of medical signals and sensors,* vol. 3, p. 45, 2013.

[10] S. C. Huynh, X. Y. Wang, G. Burlutsky, and P. Mitchell, "Symmetry of optical coherence tomography retinal measurements in young children," *American journal of ophthalmology,* vol. 143, pp. 518-520, 2007.

[11] J. J. Park, D. R. Oh, S. P. Hong, and K. W. Lee, "Asymmetry analysis of the retinal nerve fiber layer thickness in normal eyes using optical coherence tomography," *Korean Journal of Ophthalmology,* vol. 19, pp. 281-287, 2005.

[12] T. Mahmudi, R. Kafieh, H. Rabbani, and M. Akhlagi, "Comparison of macular OCTs in right and left eyes of normal people," in *SPIE Medical Imaging*, 2014, pp. 90381W-90381W-6.

[13] S. Asrani, J. A. Rosdahl, and R. R. Allingham, "Novel software strategy for glaucoma diagnosis: asymmetry analysis of retinal thickness," *Archives of ophthalmology,* vol. 129, pp. 1205-1211, 2011.

[14] Y. Kurimoto, K. Matsuno, Y. Kaneko, J. Umihira, and N. Yoshimura, "Asymmetries of the retinal nerve fibre layer thickness in normal eyes," *British journal of ophthalmology,* vol. 84, pp. 469-472, 2000.

[15] E. A. Essock, M. J. Sinai, and R. D. Fechtner, "Interocular symmetry in nerve fiber layer thickness of normal eyes as determined by polarimetry," *Journal of glaucoma,* vol. 8, pp. 90-98, 1999.

[16] J.-C. Mwanza, M. K. Durbin, D. L. Budenz, and C. O. N. D. S. Group, "Interocular symmetry in peripapillary retinal nerve fiber layer thickness measured with the Cirrus HD-OCT in healthy eyes," *American J of Ophth.,* vol. 151, pp. 514-521. e1, 2011.

[17] D. L. Budenz, "Symmetry between the right and left eyes of the normal retinal nerve fiber layer measured with optical coherence tomography (an AOS thesis)," *Transactions of the American Ophthalmological Society,* vol. 106, p. 252, 2008.

[18] E. Larsson, U. Eriksson, and A. Alm, "Retinal nerve fibre layer thickness in full-term children assessed with Heidelberg retinal tomography and optical coherence tomography: normal values and interocular asymmetry," *Acta ophthalmologica,* vol. 89, pp. 151-158, 2011.

[19] D. J. Salchow, Y. S. Oleynikov, M. F. Chiang, S. E. Kennedy-Salchow, K. Langton, J. C. Tsai*, et al.*, "Retinal nerve fiber layer thickness in normal children measured with optical coherence tomography," *Ophthalmology,* vol. 113, pp. 786-791, 2006.

[20] C. Al-Haddad, R. Antonios, and H. Tamim, "Interocular symmetry in retinal and optic nerve parameters in children as measured by spectral domain optical coherence tomography," *British Journal of Ophthalmology,* pp. bjophthalmol-2013-304345, 2014.

[21] J. D. Dalgliesh, Y. M. Tariq, G. Burlutsky, and P. Mitchell, "Symmetry of retinal parameters measured by spectral-domain OCT in normal young adults," *Journal of glaucoma,* vol. 24, pp. 20-24, 2015.

[22] M. S. Alluwimi, W. H. Swanson, and V. E. Malinovsky, "Between-Subject Variability in Asymmetry Analysis of Macular Thickness," *Optometry & Vision Science,* vol. 91, pp. 484-490, 2014.

[23] Y. CHEN, N. KOBAYASHI, and K. KOBAYASHI, "Asymmetry in hemifield macular thickness as an indicator of early glaucomatous structural or functional progression," *Acta Ophthalmologica,* vol. 90, pp. 0-0, 2012.

[24] H. Yamada, M. Hangai, N. Nakano, K. Takayama, Y. Kimura, M. Miyake*, et al.*, "Asymmetry Analysis of Macular Inner Retinal Layers for Glaucoma Diagnosis," *American journal of ophthalmology,* vol. 158, pp. 1318-1329. e3, 2014.

[25] I. Liberek, S. Chaberek, E. Anielska, K. Kowalska, and K. Ostrowski, "Symmetry of retinal vessel arborisation in normal and amblyopic eyes," *Ophthalmologica,* vol. 224, pp. 96-102, 2009.

[26] R. Kolar and P. Tasevsky, "Registration of 3D retinal optical coherence tomography data and 2D fundus images," in *Biomedical Image Registration*, ed: Springer, 2010, pp. 72-82.

[27] B. Zitova and J. Flusser, "Image registration methods: a survey," *Image and vision computing,* vol. 21, pp. 977-1000, 2003.

[28] A. Soltanipour, S. Sadri, H. Rabbani, M. Akhlaghi, and A. Doost-Hosseini, "Vessel centerlines extraction from Fundus Fluorescein Angiogram based on Hessian analysis of directional curvelet subbands," in *2013 IEEE Int. Conference on Acoustics, Speech and Signal Processing (ICASSP),* 2013, pp. 1070-1074.

[29] D. L. Donoho and M. R. Duncan, "Digital curvelet transform: strategy, implementation, and experiments," in *AeroSense 2000*, 2000, pp. 12-30.

[30] C. Li, C. Xu, C. Gui, and M. D. Fox, "Distance regularized level set evolution and its application to image segmentation," *Image Processing, IEEE Transa. on,* vol. 19, pp. 3243-3254, 2010.

[31] Y.-p. Wang, Q. Chen, and S.-t. Lu, "Quantitative assessments of cup-to-disk ratios in spectral domain optical coherence tomography images for glaucoma diagnosis," *2013 6th Int. Conference on* in *Biomedical Engineering and Informatics (BMEI),* 2013, pp. 160-165.

[32] SH. Hajeb, H. Rabbani, MR. Akhlaghi, "A new combined method based on curvelet transform and morphological operators for automatic detection of foveal avascular zone", *Signal, Image & Video Processing*, vol. 8, no. 2, pp. 205-222, Feb. 2014.

[33] M. V. Afonso, J. M. Bioucas-Dias, and M. A. T. Figueiredo. "Fast image recovery using variable splitting and constrained optimization", *IEEE Trans. Image Process*., vol. 19, no. 9, pp. 2345-2356, Sept. 2010.